Cytotoxic Origin of Copper(II) Oxide Nanoparticles: Comparative Studies with Micron-Sized Particles, Leachate, and Metal Salts

ARTICLE *in* ACS NANO · AUGUST 2011

Impact Factor: 12.88 · DOI: 10.1021/nn2020248 · Source: PubMed

Cytotoxic Origin of Copper(II) Oxide Nanoparticles: Comparative Studies with Micron-Sized Particles, Leachate, and Metal Salts

Cindy Gunawan,[†] Wey Yang Teoh,[‡] Christopher P. Marquis,[§] and Rose Amal[†,*]

[†]ARC Centre of Excellence for Functional Nanomaterials, School of Chemical Engineering, The University of New South Wales, Sydney, NSW 2052, Australia, [‡]School of Energy and Environment, City University of Hong Kong, Hong Kong Science Park, Shatin, N.T., Hong Kong, and [§]School of Biotechnology and Biomolecular Sciences, The University of New South Wales, Sydney, NSW 2052, Australia

ABSTRACT The work investigates the source of toxicity of copper oxide nanoparticles (CuO NPs) with respect to its leaching characteristic and speciation. Complexation-mediated leaching of CuO NPs by amino acids was identified as the source of toxicity toward *Escherichia coli*, the model microorganism used in the current study. The leached copper—peptide complex induces a multiple-fold increase in intracellular reactive oxygen species generation and reduces the fractions of viable cells, resulting in the overall inhibition of biomass growth. The cytotoxicity of the complex leachate is however different from that of equivalent soluble copper salts (nitrates and sulfates). A pH-dependent copper speciation during the addition of copper salts gives rise to uncoordinated copper ions, which in turn result in greater toxicity and cell lysis, the latter of which was not observed for CuO NPs even at comparable pH. Since leaching did not occur with micrometer-sized CuO, no cytotoxicty effect was observed, thus highlighting the prominence of materials toxicity at the nanoscale.

KEYWORDS: nanoparticle · nanotoxicology · bacteria proliferation · leaching · metal salts · reactive oxygen species

Copper oxide, alongside other inorganic materials such as silver (metallic and oxide) and zinc oxide are among the most widely applied antimicrobial agents. With proven efficacy toward various microorganisms including yeast,[1] algae,[2] bacteria,[3] and even viruses,[4] the exploitation of copper oxide ranges widely from wood preservation,[5] antifouling paints, to antibacterial textiles.[6] In its nano form (<100 nm), copper oxide displays enhanced antimicrobial activity toward a broad spectrum of microorganisms, including pathogens such as *Escherichia coli* and *Staphylococcus aureus*.[7−10] While this is a highly desirable characteristic, the little-known environmental impact of copper oxide nanoparticles (CuO NPs) is a cause of concern. Hence, establishing a mechanistic understanding of the antimicrobial action of CuO NPs is one of the key challenges toward assessment of their environmental impact.

Recent studies have identified the leaching characteristics of nanoparticles as one of the key properties leading to their antimicrobial efficacy (or a wider context of nanotoxicity).[11−15] Leached nanoparticles in the form of soluble ions interact directly with the cellular membrane or are taken up intracellularly, thereby causing cytotoxicity. Alternatively, the Trojan horse effect, whereby nanoparticles are internalized and dissolved intracellularly, has been suggested.[11,16,17] An inherent complexity arises from the often overlooked materials specificity and their unique route of toxicity with respect to size-dependent physicochemical properties. It is within this context that the source of cytoxicity of CuO NPs is being studied.

The intracellular generation of reactive oxygen species (ROS), a general oxidative stress signaling mechanism in living cells,[18,19] including that of *E. coli*,[20] is often taken as a measurement of cytotoxicity. That is to say, cytotoxicity results when the natural antioxidant defense is overwhelmed by generation of excess cellular ROS induced in the presence of foreign materials, be it soluble ions or particles. To date however, the relevance of such a toxicity paradigm on environmental microorganisms is only vaguely understood.

Addressing the challenge, the current study aims to investigate the mode of toxicity of copper oxide in the form of (bulk) micrometer particles as well as nanoparticles. Parallel comparisons will also be carried out with soluble copper ions to distinguish between the role of free ions and that of the copper oxide, in conjunction

* Address correspondence to r.amal@unsw.edu.au.

Received for review June 1, 2011 and accepted August 3, 2011.

Published online August 03, 2011
10.1021/nn2020248

with its leached soluble copper. In particular, the experiments are performed under organic-rich culture medium, representing the potential environment, such as organic-rich wastewater, where microorganisms are most likely to thrive. To the best of our knowledge, the present study is the first holistic investigation on the toxicity origin of CuO NPs in relation to the physiological effects of a model microorganism.

RESULTS AND DISCUSSION

Antimicrobial Action of Copper Oxide Nanoparticles and Induced Leaching. An environmentally relevant *E. coli* is chosen as the model microorganism for the assessment of antimicrobial characteristics of CuO NPs. Figure 1a shows the extent of bacterial growth in the presence of homogeneous and highly crystalline CuO NPs (70 $m^2 g^{-1}$, d_{SSA} = 14 nm, Figure 1c and e) prepared by flame spray pyrolysis,[21,22] at various dosages of 150, 350, 480, 550, 650, and 900 mg L^{-1}. After 6 h exposure to the lowest loading of 150 mg L^{-1} CuO NPs, the biomass growth of *E. coli* was inhibited by only 10% with respect to the control experiment without CuO. Under normal circumstances, such dosage is readily lethal to other microorganisms such as the bacteria *Vibrio fischeri* and microcrustaceans *Daphnia magna* and *Thamnocephalus platyurus*.[25] The relatively high toxicity threshold of *E. coli* may be attributed to activation of the coordinated heavy-metal efflux defense system, where extracellular pumping of cytoplasmic copper is achieved *via* sequential activation of the multilevel CPx-type ATPases and RND (resistance, nodulation, and cell division) proteins, in response to increasing concentration of copper in the growth medium.[23,24] A 50% biomass growth inhibition (6 h EC_{50}) as high as 350 mg L^{-1} CuO NPs is observed in the current work for *E. coli*. At the extreme dosage of 900 mg L^{-1} CuO NPs, more than 90% growth inhibition results. As we show later, the dosage response of *E. coli* is a size-dependent function of CuO, *i.e.*, micrometer- or nano-sized particles, and that bioavailability of copper is significantly affected by the presence of organics.

In relation to the growth kinetics of *E. coli*, parallel copper dissolution was carried out throughout the course of NP exposure. As depicted in Figure 1b, leaching of CuO NPs proceeded rapidly within the first hour, with >80% of soluble copper relative to total copper detected in the culture medium containing 150−480 mg L^{-1} CuO NP exposure (corresponding to 102−315 ppm soluble Cu, respectively). A lower extent of dissolution of 60−75% was observed at the higher 550−900 mg L^{-1} loadings (corresponding to 336−445 ppm soluble Cu, respectively) in the first hour, the kinetics of which was likely to be governed by the Gibbs free energy of dissolution. Equilibrium was reached at 3 h for all tested loadings, with the extent of copper leaching >90% of total copper, regardless of the initial amount of added CuO NPs. Comparison of leaching kinetics in the absence (dashed line) and presence (solid line) of *E. coli* did not find any differences, at least within the concentrations tested, thereby ruling out any additional effects of microbial-induced leaching,[26] as has been reported for the dissolution of copper.[27]

To elucidate the high degree of CuO NP leaching, individual component leaching was carried out on the basis of the mixture of culture medium: deionized water, NaCl, tryptone, and yeast extract. As shown in Table 1, the extent of leaching is clearly affected by the presence of the organic tryptone and yeast extract, while the presence of deionized water alone or in the presence of NaCl has little effect on the dissolution of CuO NPs. In fact, the extent of leaching in the latter two components is indifferent to that of micrometer-sized CuO particles (0.7 $m^2 g^{-1}$, d_{SSA} = 4.8 μm, Figure 1d and e). In other words, the chloride-mediated leaching can be ruled out as the dissolution agent regardless of the particle size. On the contrary, a significant difference between the leaching of CuO NPs and that of micrometer-sized particles can be readily observed in the amino acid-rich components, *i.e.*, tryptone and yeast extract. Extensive copper leaching of 95% and 80% (relative to total copper dissolved in the culture medium) was measured for CuO NPs in the respective medium, while a corresponding leaching of only 2% and 1% was measured for micrometer-sized CuO. The fact that the sum of leached copper from tryptone and yeast extract alone surpasses that of the growth media indicates a competitive and nonselective leaching from each of the components. Indeed, borderline Lewis acid Cu(II) is known to form complexes with amino acids such as histidine, cysteine, and lysine due to its high affinity for the side chains.[28] On the basis of the unchanged amount of leached copper from micrometer-sized CuO after 24 h exposure in both aqueous tryptone and yeast extract, it is argued that the leaching kinetics extend beyond just surface area limitations or the shrinking core model. Instead, it is likely that the leaching is driven in part by the Kelvin effect, where the much larger surface curvature of CuO NPs induces higher affinity for the dissolution of copper, assisted by the complexation with free amino acids and peptide chains.

Importantly, as shown by the red solid line in Figure 2, the biomass growth suppression of *E. coli* exhibits a strong function with increasing amount of leached copper from CuO particles. However, the extent of suppression by the analogous addition of copper salts as nitrate or sulfate is different and separate (blue dashed line) from that of CuO particles (the mechanism of which will be discussed later). Despite establishing a clear relationship between leached copper concentration and *E. coli* biomass growth inhibition up to this juncture, the extent of the Trojan horse effect on the antimicrobial activity of

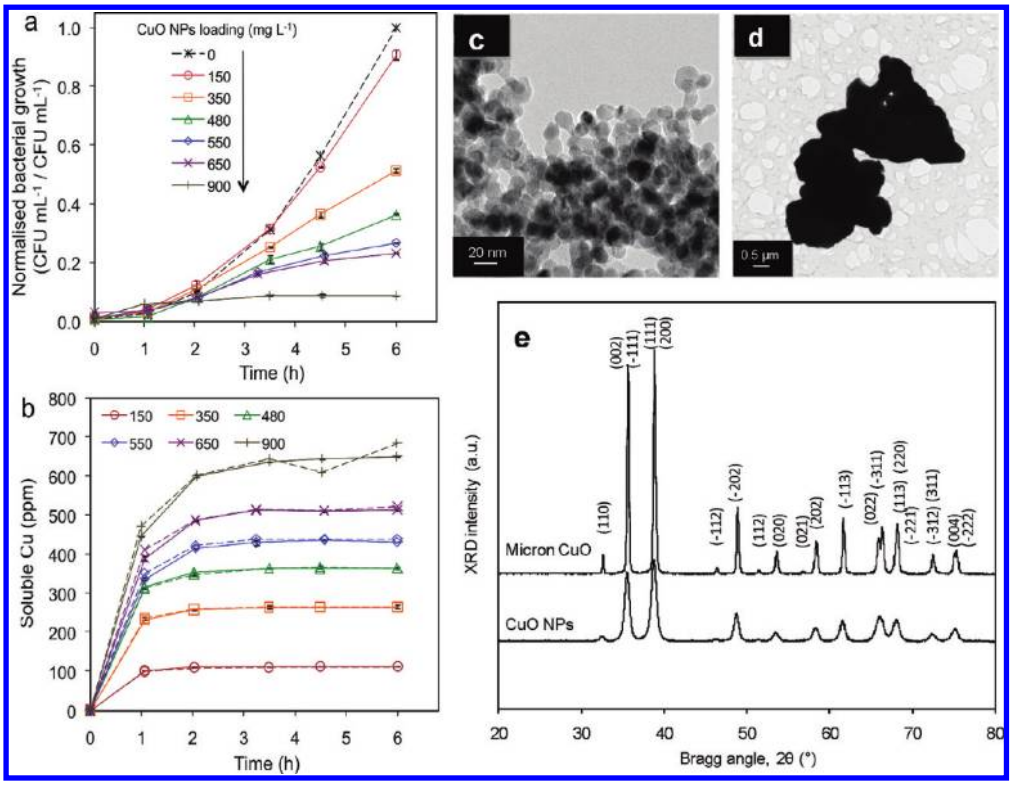

Figure 1. (a) Growth kinetics of *E. coli* in the presence of different CuO NP loadings and that of a control experiment without copper. (b) Corresponding leaching kinetics in the absence (dashed lines) and presence (solid lines) of *E. coli* in Luria–Bertani (LB) medium. The toxic effect of NPs was obtained by normalizing the extent of growth (in colony forming units, cfu) to the bacteria-only control. Each data point in (a) and (b) is the average of the triplicate batches, with error bars representing the maximum and minimum. The growth kinetic profiles were reproduced on different days with unique bacterial inoculum and particle preparations. Also shown are the transmission electron micrographs of aggregates of (c) CuO NPs and (d) micrometer-sized CuO, as well as (e) their corresponding X-ray diffraction spectra. The diffraction peaks are indexed to monoclinic CuO (PDF: 080-1268). Note the diffraction peaks of CuO NPs show significant peak broadening due to small grain size.

TABLE 1. Leaching Kinetics of Nano- and Micrometer-Sized CuO Particles in Cell-Free Individual Components of the Culture Medium (Luria–Bertani, LB)

	H_2O[b]			NaCl[c]			yeast extract[d]			tryptone[e]			culture media[f]		
	3 h	24 h	48 h	3 h	24 h	48 h	3 h	24 h	48 h	3 h	24 h	48 h	3 h	24 h	48 h
	Soluble Cu (ppm)														
CuO NPs[a]	5.7	4.7	6.4	2.5	4.1	3.9	218.9	298.8	281.5	318.9	344.7	338.7	363.8	364.1	366.2
micron CuO[a]	1.4	0.9	1.4	1.3	1.0	6.4	1.0	4.2	4.6	1.0	8.3	8.3	1.5	2.0	2.0

[a] CuO particles (480 mg L^{-1}) were incubated in the respective culture medium (LB) component in the absence of cells at 37 °C, 280 rpm. [b] Deionized water. [c] 5 g L^{-1} NaCl in aqueous. [d] 5 g L^{-1} yeast extract in aqueous. [e] 10 g L^{-1} tryptone in aqueous. [f] Culture media consists of 5 g L^{-1} NaCl, 5 g L^{-1} yeast extract, 10 g L^{-1} tryptone dissolved in deionized water. Aqueous refers to solubilization in deionized water.

CuO NPs is still not fully clear. Hence, an independent set of experiments was carried out where 480 mg L^{-1} CuO NPs was preleached in the sterilized culture medium, followed by separation of the remaining CuO solids. *Note:* The resultant amount of leached copper (365 ppm soluble Cu) corresponds exactly to that shown earlier in Figure 1b. As evident in Figure 2 (pink diamond), the biomass growth of *E. coli* under the leached copper-laden medium is comparable to that in the presence of CuO NPs at identical concentration. The observation implies the absence of a Trojan horse toxicity effect possibly due to the significant and rapid leaching nature of CuO NPs, while reaffirming the source of toxicity as originating exclusively from copper in its dissolved state.

Figure 2 (dashed line) shows the studies with soluble copper conducted through the addition of copper nitrate as well as sulfate salts. As mentioned earlier, the extent of inhibition of biomass growth induced by copper salts (6 h EC_{90} = 265 ppm Cu) is much higher than that of the CuO particles (6 h EC_{90} = 650 ppm Cu) particularly at high copper concentrations. That no observable difference in the antimicrobial activity between copper nitrate and that of sulfate suggests that the higher toxicity cannot be

accounted for by the difference in anionic species. In fact, external addition of an equivalent amount of nitrates (as sodium nitrate) to the culture medium containing preleached CuO NPs did not result in additional antimicrobial activity compared to that of CuO NPs alone (Figure 2, open diamond). At this stage, it would be reasonable to deduce that the difference in the speciation of soluble copper may have resulted in such effect. Detailed comparison of intracellular studies under these experimental conditions, as will be presented in the following sections, will provide insights into the source of cytotoxicity of copper particles and the associated leachate, as well as copper salts.

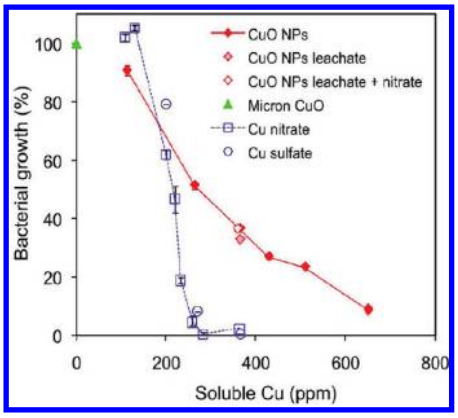

Figure 2. Dosage−response of *E. coli* growth taken at 6 h, relative to the bacteria-only control, as a function of soluble copper from CuO NPs (red solid line), leachate, micrometer-sized CuO, and copper nitrate and sulfate (blue dashed line). Also shown is the bacterial growth in the presence of CuO NPs leachate and addition of sodium nitrate (open diamond). The data for CuO NPs leachate (with and without addition of sodium nitrate), micrometer-sized CuO, and copper salts were reproduced on different days with a unique bacterial inoculum and particle or soluble copper preparations. All growth experiments were performed in triplicate.

Intracellular ROS Generation and Induced Cytotoxicity of CuO NPs, Copper Leachate, and Salt. *Ex situ* tracking of intracellular ROS generation (with the H_2DFFDA assay) and cell viability (with propidium iodide, PI, staining) was carried out throughout the course of *E. coli* growth in the presence of various forms of copper, that is, CuO NPs, filtered leachate, micrometer-sized CuO, and copper nitrate. Unless otherwise stated, 480 mg L^{-1} of CuO particles, or equivalent to 365 ppm soluble copper, is taken as the reference loading from here onward. As shown in Figures 3a and 4, the presence of CuO NPs and that of leachate induce a ~5-fold increase in ROS level compared to the base level of bacteria-only control. Under normal circumstances, exposure of living cells to environmental stresses such as metal toxicity triggers the cellular defense machinery to cope with the elevated levels of cellular ROS generation.[29,30] In particular for *E. coli*, this involves the utilization of peroxide and/or superoxide stimulons, activation of which leads to the expression of enzymatic antioxidants as ROS scavengers.[31] However, when the defense mechanism is overwhelmed, such as the current case, ROS, or more specifically peroxides and hydroxyl radicals, are generated from the redox cycling of intracellular copper catalyzed by periplasmic CuZn-superoxide dismutase (SOD1) in *E. coli*.[32−34] Other sources of copper-catalyzed ROS generation include the autoxidation of the cellular antioxidant glutathione.[35,36]

The levels of nonviable cells in samples exposed to CuO NPs and those of the leachate are almost identical (Figures 3b and 4), corroborating our earlier conclusion from the growth kinetics that the toxicity of CuO NPs originates solely from the leachate. The higher proportion of PI-positive cells in these samples relative to the

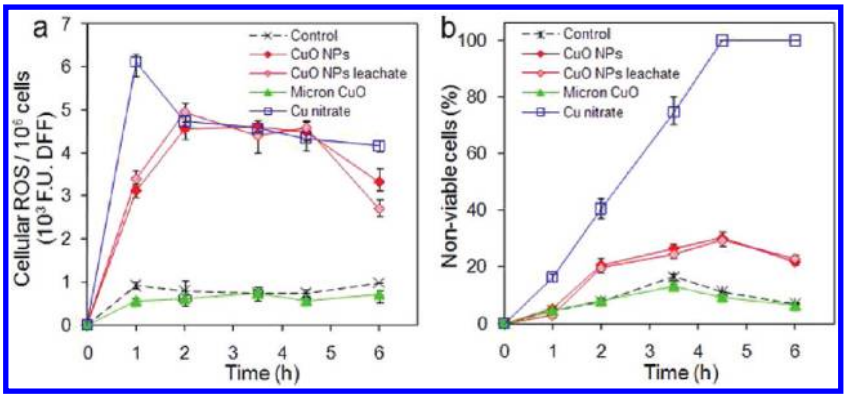

Figure 3. Dynamics of (a) intracellular ROS generation probed by the H_2DFFDA assay and (b) cell viability probed by PI staining, throughout the course of growth of *E. coli* in the presence of CuO NPs, micrometer-sized CuO, leachate from CuO NPs, and copper nitrate. The concentration of CuO particles (CuO NPs, micrometer CuO) was 480 mg L^{-1}. The soluble copper concentration in leachate and copper nitrate was 365 ppm, corresponding to the steady-state soluble copper concentration from 480 mg L^{-1} CuO NPs. Also shown is the bacteria-only control (dashed line). The data points are the average of three repeated experiments, each with different days of bacterial inoculum and particle or soluble copper preparations. Error bars represent the maximum and minimum. Unpaired two-tailed Student's *t*-test with unequal variance was used for statistical analysis. The test confirms elevated cellular ROS levels and increased fraction of dead cells with CuO NP-, leachate-, and copper nitrate-treated cells relative to the control with $p < 0.05$, 0.025, 0.01, and 0.005 (see Figure S1 in the Supporting Information).

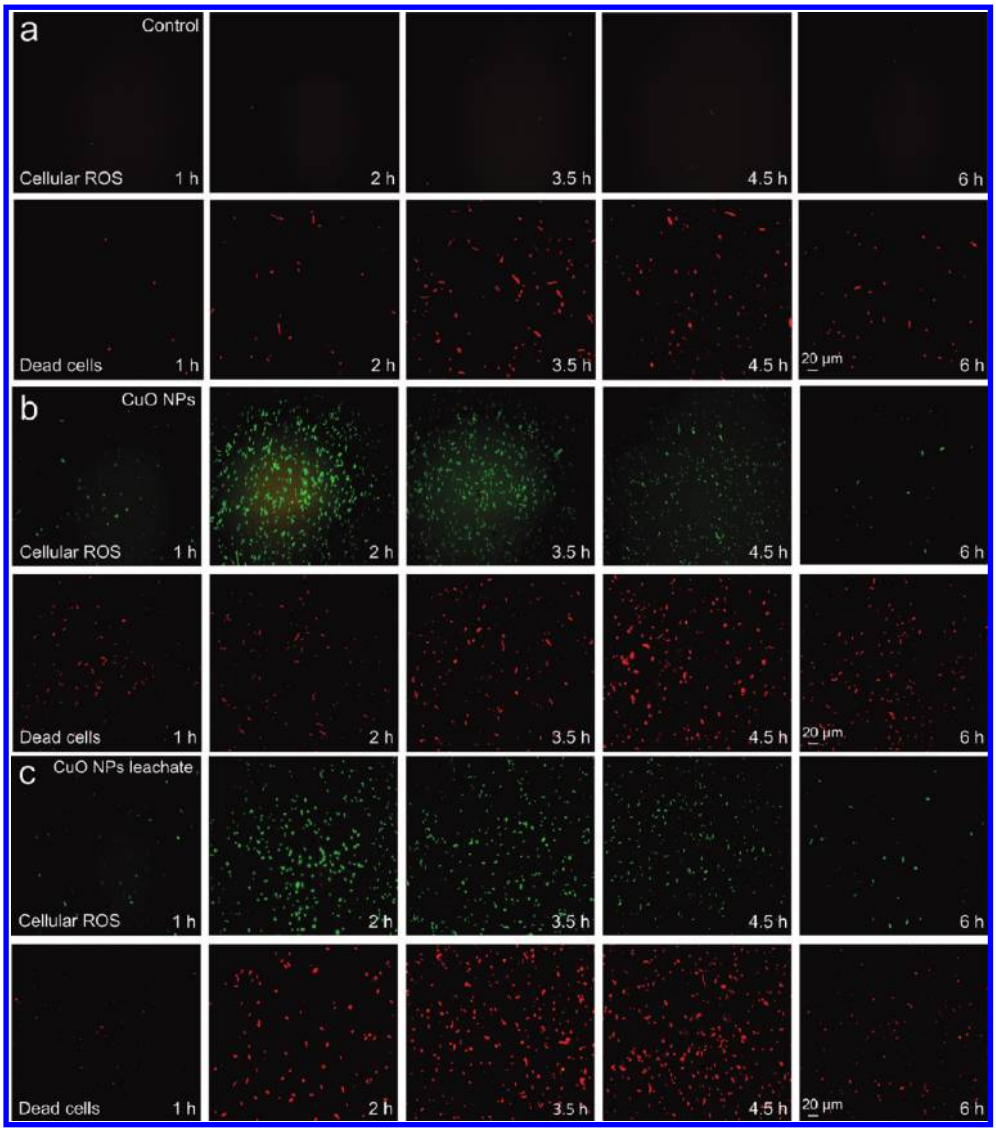

Figure 4. Detection of intracellular ROS generation (measured with H_2DFFDA staining, green) and cell death (PI staining, red) of *E. coli* over its course of growth (a) in the absence of copper, (b) with exposure to 480 mg L^{-1} of CuO NPs, and (c) with exposure to equivalent copper leachate (365 ppm soluble Cu) from CuO NPs. All stained samples were imaged at comparable cell concentrations.

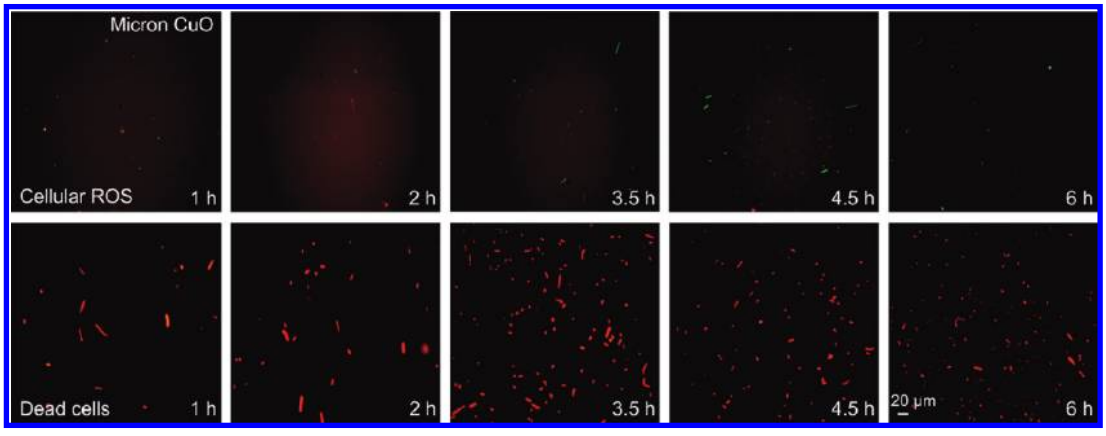

Figure 5. Detection of intracellular ROS generation (H_2DFFDA staining, green) and cell death (PI staining, red) of *E. coli* over its course of growth in the presence of 480 mg L^{-1} micrometer-sized CuO. All stained samples were imaged at comparable cell concentration.

control implies the cytoplasmic membrane as one of the target destruction sites of the copper-induced ROS. In fact, as part of the multilevel copper defense mechanism of *E. coli*, trans-membrane efflux of copper is

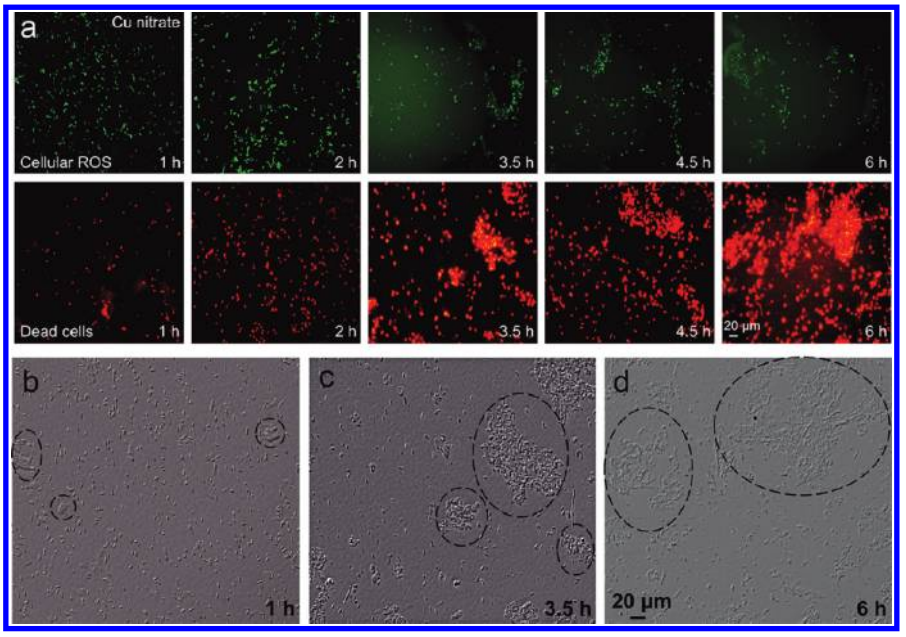

Figure 6. (a) Detection of intracellular ROS generation (H_2DFFDA staining, green) and cell death (PI staining, red) of *E. coli* over its course of growth in the presence of 365 ppm soluble Cu as copper nitrate. The amount of copper corresponds to that of the steady-state soluble copper concentration leached from 480 mg L^{-1} CuO NPs. All stained samples were imaged at comparable cell concentrations. Also shown are the light microscopy images of the bacteria population at (b) 1 h, (c) 3.5 h, and (d) 6 h. Note the higher extent of cell lysis and aggregation of dead cells with increasing exposure time.

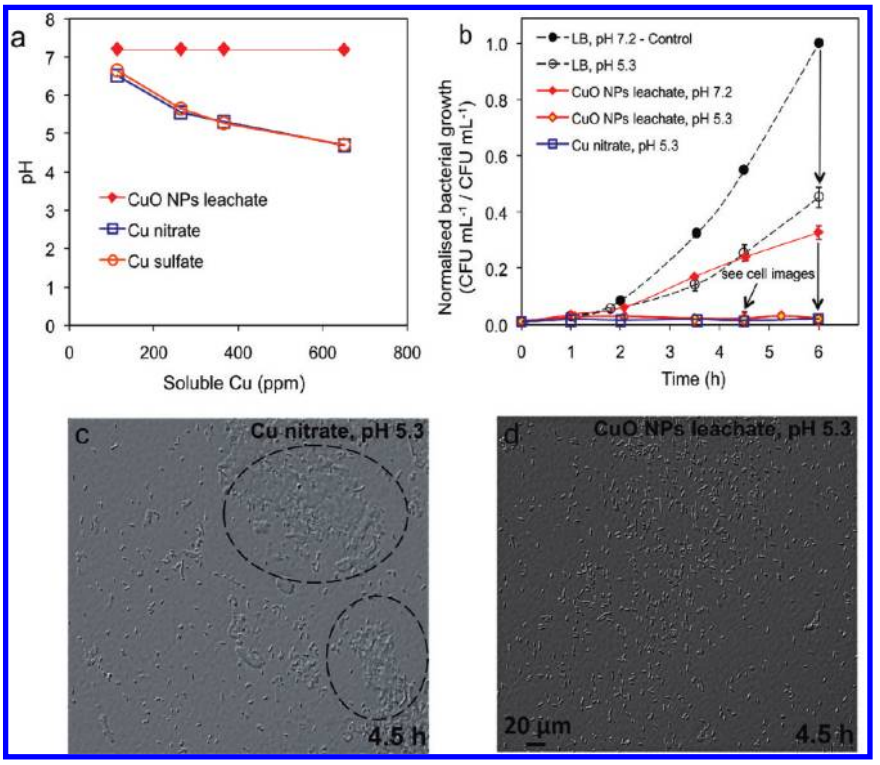

Figure 7. (a) Unadjusted pH of culture media as a function of soluble Cu loadings from leachate, copper nitrate, and sulfate. (b) Effect of acidification from pH 7.2 to 5.3 (by addition of nitric acid) on the growth kinetics of *E. coli* in pure culture media and that in the presence of 365 ppm copper leachate. Also shown is the growth kinetics of *E. coli* in the presence of copper nitrate (equivalent to 365 ppm soluble Cu), which gives pH 5.3. All growth experiments were performed in triplicate and reproduced on different days with unique bacterial inoculum and soluble copper preparations. Light microscopy shows (c) cell lysis and aggregation in the presence of copper nitrate at pH 5.3 and (d) the absence of cell lysis in copper leachate at the same pH.

facilitated *via* the action of ATPase CopA, which pumps cytoplasmic copper into the periplasm,[37,38] while the proton-driven CusCBFA system further exports the periplasmic copper across the outer membrane.[39] At

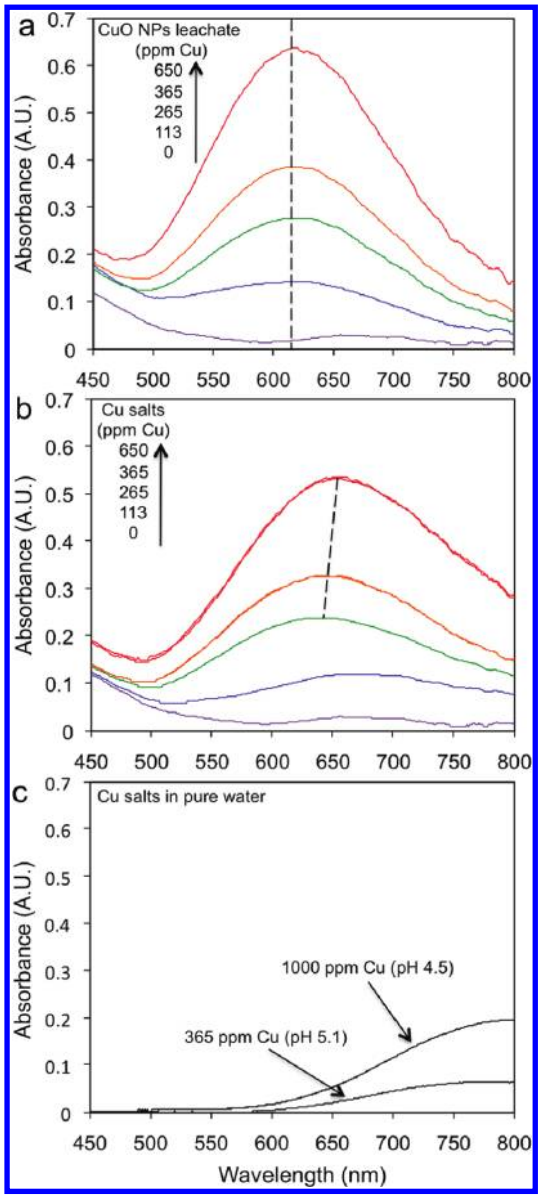

Figure 8. Visible wavelength absorption spectra as a function of soluble copper concentrations for (a) leachate from CuO NPs and (b) copper nitrate and sulfate (the latter only at 365 and 650 ppm). Note the gradual red shift of the absorption maxima (and skewing of the shoulder at higher wavelength) with increasing copper nitrate loadings, indicative of increasing concentration of uncoordinated copper species. Also shown is the (c) overlapping absorption spectra of aqueous copper nitrate and sulfate at 365 and 1000 ppm soluble copper, dominated by the presence of free Cu^{2+} (and $Cu(OH)^{+}$) ions.

elevated copper exposure, substantial hydroxyl radical formation and localization of H_2O_2-oxidizable copper in the periplasm has been suggested in *E. coli*.[40] Herein, we do not rule out the possibility of cellular uptake of soluble copper, which amounts to $\sim 10^{-4}$ μmol at the highest *E. coli* population, assuming the maximum homeostasis condition of 100 μM in each cell.[24] This upper limit of copper uptake is 3 orders of magnitude below the detection limit of soluble copper in the current work and hence is not contradictory to the indifferent copper leaching profiles in the absence or presence of *E. coli* (Figure 1b). Apart from the observed lethal effects, the copper-induced ROS generation may also inflict sublethal cellular damage, leaving a significant population of the viable cells uncultivable or sluggishly proliferating. This is further verified by our growth kinetics prediction based on the fraction of viable cells, *i.e.*, $[A_n] = [A_{n-1}] \times e^{kt}$, where $[A_{n-1}]$ is the concentration of PI-negative cells at the previous time interval, and it clearly overestimates the actual course of *E. coli* growth in the presence of soluble copper (see Figure S2 in the Supporting Information). ROS, or more specifically H_2O_2-treated *E. coli*, is known to adopt the nonproliferating bacteriostatic state due to the stimulation of DNA strand cleavage.[41,42] Base excision repair as mediated by DNA polymerase I would normally follow at the expense of inhibition of DNA replication by polymerase III.[43] Such sequential events may explain the impaired proliferation of *E. coli* at elevated ROS level.

Exposure to micrometer-sized CuO, due to its low amount of copper leaching, did not result in additional ROS generation relative to the control (Figures 3 and 5). This consolidates the nontoxicity of micrometer-sized CuO toward *E. coli*. Similarly, the fraction of viable cells was similar to that of the control experiment over the entire course of growth.

Rapid cellular ROS generation in *E. coli* can be observed within the first hour of exposure to copper nitrate, which is almost twice that observed for CuO NPs and its corresponding leachate (Figures 3a and 6). In the subsequent hours, the apparent cellular ROS level was comparable to that of the CuO NPs and its leachate. However, closer inspection of Figure 6 finds cytolysis of cells and release of cellular materials beyond the first hour, resulting in aggregation of the ruptured cells (highlighted in circled regions). The extent of aggregation, most likely induced by the hybridization of plasmid DNA from ruptured cellular materials,[44,45] becomes more significant at increased exposure time due to the higher population of more lysed cells. Because of the effect of aggregation, underestimation of the ROS-positive cell population may be inevitable during the flow cytometry measurement, since only single cells and possibly small cell aggregates are detected in the analysis, leaving the larger aggregates unaccounted. The same applies to the cell viability assessment (Figure 3b), which nonetheless may still be valid qualitative evidence to show the higher fraction of nonviable cells associated with copper nitrate compared to that of CuO NPs at all time exposures. *E. coli* when subjected to severe stress conditions, including an ultimate oxidative stress, triggers the "suicide" toxin–antitoxin *mazEF* chromosomal genetic module, thereby initiating programmed cell death.[46,47] Such ROS-linked cytolysis had also been observed in the cinnamaldehyde-treated cyanobacteria *Microcystis aeruginosa* as well as AgCl-treated

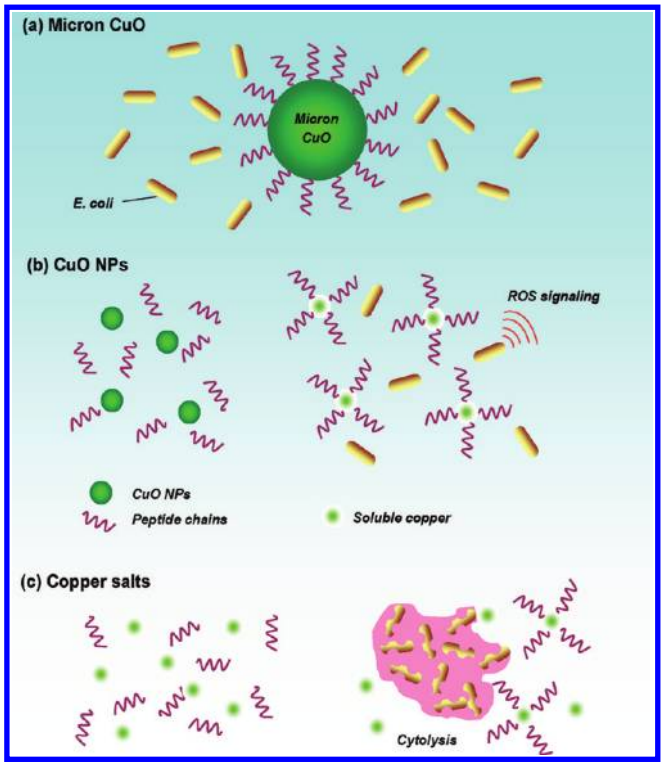

Scheme 1. Proposed mechanism of the interactions of (a) micrometer-sized CuO, (b) CuO NPs, and (c) copper salts with an organic-rich environment, containing free peptide chains, and their toxic effects on bacteria.

E. coli.[48,49] In the current work, essentially all copper nitrate (and copper sulfate)-exposed cells became nonviable at 4.5 h. The much higher cytotoxicity effect of copper salt corroborates the higher extent of suppressed biomass growth. As we further show in the next section, the difference in the copper speciation of leached copper and that of the salt was critical to the fundamental cytotoxicity effect of copper.

Effects of pH and Copper Speciation on the Cytotoxicity of Soluble Copper. As a result of the acidic nature of copper salts (as nitrate and sulfate), their addition inevitably decreases the pH of the culture medium from pH ~7.2 (without copper) to pH 5.3 (at 365 ppm soluble Cu) (Figure 7a). The resultant pH is detrimental to the proliferation of *E. coli*, as would be expected for acidic medium of pH <6.5. Leaching of CuO NPs on the other hand does not alter the pH of the solution even up to the highest loading of 900 mg L^{-1} CuO NPs (Figure 7a). This is true despite incubation of the particles in the medium for more than 24 h, implying that the unobserved decrease in pH of the medium and further cytotoxicity effect are unrelated to the kinetics of copper leaching and speciation. The role of copper speciation, depending on the source of soluble copper, will be discussed in detail below.

To first verify the extent of growth suppression by pH change, the growth of *E. coli* was carried out in acidified culture medium (pH 5.3 by addition of nitric acid) and in the absence of copper. As shown in Figure 7b, the biomass growth was suppressed by 55% after 6 h just by the change of pH. Further acidification of the leachate from CuO NPs almost inhibits completely the growth of *E. coli*, matching that of equivalent copper nitrate. Nevertheless, the effect of acidified copper leachate (also by addition of nitric acid) was clearly different from that of copper nitrate. As shown from the microscopy examination in Figure 7c and d, while the latter resulted in cytolysis and aggregation of ruptured *E. coli* (as discussed in the previous section), the acidification of the leachate did not result in the same effect. In other words, the findings show a stronger cytotoxicity of the dissolved copper from the copper salt, in comparison to the nanoparticle-derived leached copper, even at comparable acidic pH.

The absorption spectra of CuO NP leachate at various tested concentrations show intense blue absorption at λ_{max}= 608 nm (Figure 8a), resembling type I blue copper−protein complexes.[50] The absorbance is associated with $S_{1p\pi} \rightarrow Cu\ 3d_{x^2-y^2}$ charge transfer, which occurs when a strong Cu−S bond (for example plastocyanin, a copper-bearing electron transfer protein) in the trigonal-pyramidal coordination alters the orientation and therefore intersects the lobes of the Cu $d_{x^2-y^2}$ orbital.[51] Recalling the complexation-mediated high extent of CuO NP leaching, this is most likely to arise from copper coordination with amino acid side chains including the donor ligands from Asp and Glu ($-COO^-$), Lys ($-NH_3^+$), Arg ($-NH_2^+$), His ($-NH^+$), and cysteine ($-S^-$).[52] Despite the formation of copper−peptide

complexes, it is capable of triggering cellular oxidative stress and causing cytotoxicity, although with much less lethal response compared to copper salts.

As compared to copper leachate, the absorbance of copper salts (nitrate and sulfate) in culture medium is at lower energy and gradually shifts from λ_{max}= 645 to 662 nm with increasing copper salt loadings (Figure 8b). The red shift indicates the presence of uncoordinated copper ions, which in turn is highly pH dependent. Free Cu^{2+} and hydroxo $Cu(OH)^{+}$ ions exist in equilibrium in aqueous solutions (copper(II) hydroxide, pK_{b1} = 13, pK_{b2} = 6.3), with the former being the predominant species at low pH.[53] Because the solution pH of the culture medium decreases (pH 5.6–4.7) with increasing copper salt content (corresponding to 265–650 ppm soluble Cu, respectively), the absorbance of copper hence red shifts accordingly. The coexistence of uncoordinated copper ions and copper–peptide complexes in an organic-rich environment is thermodynamically feasible, as recently demonstrated by the detection of free Cu^{2+} in amino acid- and carbohydrate-containing culture medium following the addition of copper sulfate.[54] Interestingly, the absorbance of acidified CuO NPs leachate (from pH 7.2 to 5.3) did not exhibit a red shift despite the lowering of the pH (Figure S3 in the Supporting Information). This implies the irreversibility of the copper–peptide complexes and in turn explains the absence of cell lysis, which is most likely to be a result of exposure to the free Cu^{2+} and hydroxo $Cu(OH)^{+}$ ions. Free copper ions are capable of inducing catalytic redox cycles in biological systems leading to the generation of ROS such as hydroxyl and superoxide radicals (Scheme 1).[20,35,36] In the case of CuO NPs, the exclusive leaching by amino acids and their peptide side chains as well as its irreversibility minimizes the formation of uncoordinated copper ions (Scheme 1). The passivation of amino acids around the leached copper ions renders their lower cytotoxic effects.

CONCLUSIONS

The study sheds light on the origin of environmental nanotoxicity of copper oxide, CuO. The toxicity or antimicrobial effect is traced to the leaching of CuO NPs in amino acid-rich medium through formation of copper–peptide complexes, rather than by the solid particles themselves. The leachate from CuO NPs induces the same level of oxidative stress and cytotoxicity on *E. coli* as that in the presence of CuO NPs. The effect of leachate from CuO NPs is however different from that by addition of copper salts as nitrate or sulfate, despite having identical soluble copper concentrations. Because the leachate from CuO NPs was exclusively copper–peptide complexes, it is less cytotoxic compared to uncoordinated copper ions formed by addition of copper salts. Similar leaching did not take place on micrometer-sized CuO and is hence benign. The absence of leaching with micrometer-sized CuO implies the importance of size-related Kelvin effect on the leaching of nanoparticles. In relation to the potential environmental implications of the CuO NPs, high observable dissolution in amino acid-rich medium implies high toxicity in organic-loaded waterways, while minor leaching should be expected in freshwater or salty aquatic environments. Importantly, we demonstrate through the current work that the effect of nanoparticle leaching cannot be simply represented by the addition of metal salts. Particularly in the case of metal salt addition, the distinct cellular response is also driven by the associated pH change of the medium. The work is expected to instigate a more holistic understanding of the source of toxicity from other nanomaterials beyond CuO.

EXPERIMENTAL SECTION

Copper Oxide Synthesis and Characterization. Copper oxide nanoparticles were synthesized in a one-step flame spray pyrolysis (FSP).[21,55,56] Liquid precursor containing 0.5 M Copper 2-ethylhexanoate (Aldrich, >99.9%) in xylene (Riedel de Haen, 96%) was delivered to the FSP nozzle at 5 mL min^{-1} by means of a syringe pump (Inotech). At the nozzle tip, the liquid precursor was dispersed by 5 L min^{-1} of dispersant O_2 (1.5 bar). The dispersed precursor droplets were ignited by a supporting oxygen–methane flame (1.5 L min^{-1} CH_4/3.2 L min^{-1} O_2) to form the primary aerosol flame. Additional 5 L min^{-1} sheath O_2 was issued from the outermost ring to support the combustion. The formed CuO aerosol nanoparticles were continuously collected on a fibreglass filter (Whatmann GF/D) with the aid of a vacuum pump (Alcatel SD Series). Commercial micrometer-sized CuO (micrometer CuO, Ajax) was used as is. Specific surface areas (SSA) of the CuO samples were analyzed by N_2 adsorption at 77 K using the BET method (Tristar, Micromeritics). Prior to measurement, the samples were pretreated at 150 °C under vacuum (VacPrep, Micromeritics) for at least an hour to remove surface-adsorbed moisture and other volatile organic impurities. X-ray diffraction spectra of the samples were collected on a Philips X'Pert MPD using Cu Kα as the radiation source (40 kV, 40 mA) and scanning from 20° to 80° with a step size of 0.026°. Imaging of the CuO samples was carried out by transmission electron microscopy on a Philips CM 200 operating at 200 kV.

Antimicrobial Evaluation on *E. coli* Proliferation. *E. coli* HB101 was cultured in a shaking incubator (Bioline) in Luria–Bertani (LB) culture medium (5 g L^{-1} yeast extract, 10 g L^{-1} tryptone, 5 g L^{-1} NaCl) at 37 °C, 280 rpm under dark conditions. Bacterial inoculum was prepared by overnight culturing at 30 °C and 280 rpm from a single agar plate colony. A measured volume of 2–3 mL overnight culture (typical OD_{600} of 5–6) was transferred into 100 mL of fresh LB for a further 0.5 h conditioning at 37 °C, 280 rpm. For each growth experiment, preweighed dry-state CuO particulates were aseptically added into 50 mL of LB, unsonicated, similarly in the case of copper salts (nitrate and sulfate) exposures. The antimicrobial experiment was initiated by addition of 5 mL of bacterial inoculum into the particle suspension or dissolved copper salts (OD_{600} (bacteria) initial of 0.015), and the course of cell proliferation was evaluated for 6 h

at 37 °C, 280 rpm. In the case of CuO NP leachate exposure, 5 mL of inoculum was transferred into 50 mL of LB, containing 1.1× concentrated preleached CuO NPs. The leachate was prepared by aseptically incubating preweighed dry-state CuO NPs in cell-free LB at 37 °C, 280 rpm, for 6 h, unsonicated. The resultant copper leachate was filtered (0.22 μm cellulose membrane, Millipore) to remove undissolved solids (mean aggregate size = 300 ± 6 nm by dynamic light scattering, ZetaPals, Brookhaven). Removal of undissolved CuO particles was also confirmed by light scattering measurement of the filtered leachate, which revealed comparable scattered light intensity relative to LB medium only. The heterogeneous presence of suspended CuO particles in the growth medium is referred to in mg L^{-1}, while detected soluble copper is expressed in ppm to reflect its homogeneous nature. The growth experiments were performed in the dark (flasks wrapped in foil) and in triplicate with regular sampling for optical density measurement at 600 nm (OD_{600}) using a UV-vis spectrophotometer (Hitachi U-1100). There were two types of controls for each parameter: a copper-free growth control and the cell-free copper control (particulates or dissolved copper), of which the latter served as a reference to obtain the OD_{600} corresponding to the bacterial cell density. Inductively coupled plasma–optical emission spectroscopy (ICP-OES) (PerkinElmer Optima 3000DV) was employed to quantify the amount of leached copper from the CuO particulates as well as to validate the amount of dissolved copper associated with the preleached CuO NPs (particle-free) and copper salts. The absorption spectra of soluble copper (CuO NPs leachate, copper salts) were obtained with a UV-vis spectrophotometer (Varian Cary 300).

Cell Viability and Intracellular ROS Assays. The cell viability assay was based on the detection of damaged cytoplasmic membranes based on the uptake of the fluorescent dye propidium iodide (Sigma-Aldrich). The nucleic acid-sensitive dye penetrates cells with compromised membranes while being expelled by healthy cells. The cellular oxidative stress assay employed the oxidative-reporter dye 5-(and-6)-carboxy-2′,7′-dihydrodifluorofluorescein diacetate (H_2DFFDA) (Invitrogen, Molecular Probes Inc.), a fluorinated derivative of the more commonly used dichlorodihydrofluorescein diacetate (H_2DCFDA), with improved photostability.[57] The cell-permeable H_2DFFDA is deacetylated by intracellular esterases to active H_2DFF, which is readily oxidized by ROS, forming the highly fluorescent DFF. Samples of copper-exposed cultured cells were suspended in saline (8 g L^{-1} NaCl, 0.2 g L^{-1} KCl) at 2.5 × 10^8 cfu mL^{-1} following removal of the copper-containing medium to avoid potential production of the fluorescent derivative DFFDA due to the presence of the redox active copper, as in the case of $FeSO_4$.[58] The cell viability and cellular ROS assays were performed independently with 30 μM PI and 10 μM H_2DFFDA for 15 min and 2 h, respectively, at ambient temperature in the dark (induced by light, conversion of H_2DCFDA to fluorescent DCF had been observed in the absence of cells).[59]

Flow Cytometry. Fluorescent cell population was counted using a Cell Lab Quanta SC flow cytometer (Beckman and Coulter) at 488 nm excitation, 18 mW laser with the trigger set on the cellular electronic volume reaching 20 000 counts. PI and DFF fluorescence was detected using FL-2 and Fl-1 channel, respectively. Gain and PMT (photomultiplier tube) voltage settings were finely tuned to achieve optimal separation in the relative fluorescence intensity compared to the unstained bacterial samples. Cell Lab Quanta SC MPL software was used for data collection and gate settings. In the case where there was a high extent of cell lysis, complete cell death was further confirmed by microscopic examination (see below). Proportional to the levels of intracellular ROS, DFF fluorescence was also measured using an f_{max} microplate reader (Molecular Devices) at 485 and 538 nm excitation and emission filter settings, respectively. The ROS levels were expressed as absolute fluorescent units of the oxidized dye, DFF per 10^6 cells. Cell samples were thoroughly washed with saline (8 g L^{-1} NaCl, 0.2 g L^{-1} KCl) prior to analysis.

Microscopy Imaging. Following the staining process, cell samples were centrifuged for dye removal. Stained cells were visualized with a BX51WI fluorescence microscope (Olympus) equipped with 460–490 nm excitation filter setting and DP71 digital camera and DP-BSW software for image acquisition.

Acknowledgment. The authors acknowledge the assistance of J. Wei for flow cytometry analysis and Ricardo, Lifia, D. Oscar, and H. Limbri for their contribution in growth kinetic studies and microscopy imaging. The work was carried out with the financial support of the ARC Centre of Excellence for Functional Nanomaterials and UNSW Faculty of Engineering Early Career Researcher Grant.

Supporting Information Available: Statistical analysis of copper-induced intracellular ROS generation and cytotoxicity, first-order kinetic prediction of *E. coli* growth in the presence of CuO NPs in comparison to the actual proliferation, and visible wavelength absorption spectra (450–800 nm) of acidified CuO NP leachate, in comparison to leachate at pH 7.2 and copper salts. This material is available free of charge *via* the Internet at http://pubs.acs.org.

REFERENCES AND NOTES

1. Kasemets, K.; Ivask, A.; Dubourguier, H. C.; Kahru, A. Toxicity of Nanoparticles of ZnO, CuO and TiO_2 to Yeast *Saccharomyces cerevisiae*. *Toxicol. in Vitro* **2009**, *23*, 1116–1122.
2. Aruoja, V.; Dubourguier, H. C.; Kasemets, K.; Kahru, A. Toxicity of Nanoparticles CuO, ZnO and TiO_2 to Microalgae *Pseudokirchneriella subcapitata*. *Sci. Total Environ.* **2009**, *407*, 1461–1468.
3. Anyaogu, K. C.; Fedorov, A. V.; Neckers, D. C. Synthesis, Characterization, and Antifouling Potential of Functionalized Copper Nanoparticles. *Langmuir* **2008**, *24*, 4340–4346.
4. Borkow, G.; Zhou, S. S.; Page, T.; Gabbay, J. A. Novel Anti-Influenza Copper Oxide Containing Respiratory Face Mask. *PLoS One* **2010**, e11295.
5. Cox, C. Cromated Copper Arsenate. *J. Pestic. Reform* **1991**, *11*, 2–6.
6. Gabbay, J.; Borkow, G.; Mishal, J.; Magen, E.; Zatcoff, R.; Shemer-Avni, Y. Copper Oxide Impregnated Textiles with Potent Biocidal Activities. *J. Ind. Text.* **2006**, *35*, 323–335.
7. Paschoalino, M.; Guedes, N. C.; Jardim, W.; Mielczarski, E.; Mielczarski, J. A.; Bowen, P.; Kiwi, J. Inactivation of *E. coli* Mediated by High Surface Area CuO Accelerated by Light Irradiation >360 nm. *J. Photochem. Photobiol. A: Chem.* **2008**, *199*, 105–111.
8. Hu, X.; Cook, S.; Wang, P.; Hwang, H. M. *In vitro* Evaluation of Cytotoxicity of Engineered Metal Oxide Nanoparticles. *Sci. Total Environ.* **2009**, *407*, 3070–3072.
9. Ren, G.; Hu, D.; Cheng, E. W. C.; Vargas-Reus, M. A.; Reip, P.; Allaker, R. P. Characterisation of Copper Oxide Nanoparticles for Antimicrobial Applications. *Int. J. Antimicrob. Agents* **2009**, *33*, 587–590.
10. Perelshtein, I.; Applerot, G.; Perkas, N.; Wehrschuetz-Sigl, E.; Hasmann, A.; Guebitz, G.; Gedanken, A. CuO-Cotton Nanocomposite: Formation, Morphology, and Antibacterial Activity. *Surf. Coat. Technol.* **2009**, *204*, 54–57.
11. Xia, T.; Kovochich, M.; Liong, M.; Mädler, L.; Gilbert, B.; Shi, H.; Yeh, J. I.; Zink, J. I.; Nel, A. E. Comparison of the Mechanism of Toxicity of Zinc Oxide and Cerium Oxide Nanoparticles Based on Dissolution and Oxidative Stress Properties. *ACS Nano* **2008**, *2*, 2121–2134.
12. Navarro, E.; Piccapietra, F.; Wagner, B.; Marconi, F.; Kaegi, R.; Odzak, N.; Sigg, L.; Behra, R. Toxicity of Silver Nanoparticles to *Chlamydomonas reinhardtii*. *Environ. Sci. Technol.* **2008**, *42*, 8959–8964.
13. Sotiriou, G. A.; Pratsinis, S. E. Antibacterial Activity of Nanosilver Ions and Particles. *Environ. Sci. Technol.* **2010**, *44*, 5649–5654.
14. Li, M.; Pokhrel, S.; Jin, X.; Mädler, L.; Damoiseaux, R.; Hoek, E. M. V. Stability, Bioavailability, and Bacterial Toxicity of ZnO and Iron-Doped ZnO Nanoparticles in Aquatic Media. *Environ. Sci. Technol.* **2011**, *45*, 755–761.

15. Gunawan, C.; Teoh, W. Y.; Marquis, C. P.; Lifia, J.; Amal, R. Reversible Antimicrobial Photoswitching in Nanosilver. *Small* **2009**, *5*, 341–344.
16. Marcel, T.; Geesje, D.-T.; Maarten-Jan, C. Trojan Horse Hypothesis: Inhaled Airborne Particles, Lipid Bullets and Atherogenesis. *J. Am. Med. Assoc.* **2006**, *295*, 2354–2355.
17. Limbach, L. K.; Wick, P.; Manser, P.; Grass, R. N.; Bruinink, A.; Stark, W. J. Exposure of Engineered Nanoparticles to Human Lung Epithelial Cells: Influence of Chemical Composition and Catalytic Activity on Oxidative Stress. *Environ. Sci. Technol.* **2007**, *41*, 4158–4163.
18. Colvin, V. L. The Potential Environmental Impact of Engineered Nanomaterials. *Nat. Biotechnol.* **2003**, *21*, 1166–1170.
19. Nel, A.; Xia, T.; Mädler, L.; Li, N. Toxic Potential of Materials at the Nanolevel. *Science* **2006**, *311*, 622–627.
20. Santo, C. E.; Taudte, N.; Nies, D. H.; Grass, G. Contribution of Copper Ion Resistance to Survival of *Escherichia coli* on Metallic Copper Surfaces. *Appl. Environ. Microbiol.* **2008**, *74*, 977–986.
21. Teoh, W. Y.; Amal, R.; Mädler, L. Flame Spray Pyrolysis: An Enabling Technology for Nanoparticles Design and Fabrication. *Nanoscale* **2010**, *2*, 1324–1347.
22. Kydd, R.; Teoh, W. Y.; Scott, J.; Ferri, D.; Amal, R. Probing Surface Properties and Reaction Intermediates during Heterogeneous Catalytic Oxidation of Acetaldehyde. *ChemCatChem* **2009**, *1*, 286–294.
23. Paulsen, I. T.; Brown, M. H.; Skurray, R. A. Proton-Dependent Multidrug Efflux Systems. *Microbiol. Rev.* **1996**, *60*, 575–608.
24. Finney, L. A.; O'Halloran, T. V. Transition Metal Speciation in the Cell: Insights from the Chemistry of Metal Ion Receptors. *Science* **2003**, *300*, 931.
25. Heinlaan, M.; Ivask, A.; Blinova, I.; Dubourguier, H. C.; Kahru, A. Toxicity of Nanosized and Bulk ZnO, CuO and TiO_2 to Bacteria *Vibrio fischeri* and Crustaceans *Daphnia magna* and *Thamnocephalus platyurus*. *Chemosphere* **2008**, *71*, 1308–1316.
26. Torma, A. E.; Gabra, G. G. Oxidation of Stibnite by *Thiobacillus ferrooxidants*. *Antonie Van Leeuwenhoek* **1977**, *43*, 1–6.
27. Critchley, M. M.; Cromar, N. J.; McClure, N.; Fallowfield, H. J. The Effect of Distribution System Biofilm Bacteria on Copper Concentrations in Drinking Water. *Water Sci. Technol.* **2001**, *1*, 247–252.(Erratum: Water Supply. *Water. Sci. Technol.* **2001**, *2*, 319−324.)
28. Osterberg, R.; Sjoberg, B. Copper (I) and Copper (II) Complexes in Solution and the Crystalline State. *J. Am. Oil Chem. Soc.* **1971**, *48*, 525–526.
29. Foyer, C. H.; Noctor, G. Oxidant and Antioxidant Signaling in Plants: A Re-Evaluation of the Concept of Oxidative Stress in a Physiological Context. *Plant Cell Environ.* **2005**, *28*, 1056–1071.
30. Leonard, S. S.; Harris, G. K.; Shi, X. L. Metal-induced Oxidative Stress and Signal Transduction. *Free Radical Biol. Med.* **2004**, *37*, 1921–1942.
31. Farr, S. B.; Kogoma, T. Oxidative Stress Responses in *Escherichia coli* and *Salmonella typhimurium*. *Microbiol. Rev.* **1991**, *55*, 561–585.
32. Hodgson, E. K.; Fridovich, I. The Interaction of Bovine Erythrocyte Superoxide Dismutase with Hydrogen Peroxide: Inactivation of the Enzyme. *Biochemistry* **1975**, *14*, 5294–5299.
33. Benov, L. T.; Fridovich, I. *Escherichia coli* Expresses a Copper- and Zinc-Containing Superoxide Dismutase. *J. Biol. Chem.* **1994**, *269*, 25310–25314.
34. Gort, A. S.; Ferber, D. M.; Imlay, J. A. The Regulation and Role of the Periplasmic Copper, Zinc Superoxide Dismustase of *Escherichia coli*. *Mol. Microbiol.* **1999**, *32*, 179–191.
35. Albro, P. W.; Corbett, J. T.; Schroeder, J. L. Generation of Hydrogen Peroxide by Incidental Metal Ion-Catalyzed Autooxidation of Glutathione. *J. Inorg. Biochem.* **1986**, *27*, 191–203.
36. Misra, H. P. Generation of Superoxide Free Radical during the Autoxidation of Thiols. *J. Biol. Chem.* **1974**, *249*, 2151–2155.
37. Rensing, C.; Fan, B.; Sharma, R.; Mitra, B.; Rosen, B. P. CopA: an *Escherichia coli* Cu(I)-Translocating P-type ATPase. *Proc. Natl. Acad. Sci. U. S. A.* **2000**, *97*, 652–656.
38. Outten, F. W.; Huffman, D. L.; Hale, J. A.; O'Halloran, T. V. The Independent *cue* and *cus* Systems Confer Copper Tolerance during Aerobic and Anaerobic Growth in *Escherichia coli*. *J. Biol. Chem.* **2001**, *276*, 30670–30677.
39. Franke, S.; Grass, G.; Rensing, C.; Nies, D. H. Molecular Analysis of the Copper-Transporting Efflux System CusCFBA of *Escherichia coli*. *J. Bacteriol.* **2003**, *185*, 3804–3812.
40. Macomber, L.; Rensing, C.; Imlay, J. A. Intracellular Copper Does Not Catalyze the Formation of Oxidative DNA Damage in *Escherichia coli*. *J. Bacteriol.* **2007**, *189*, 1616–1626.
41. Imlay, J. A.; Linn, S. DNA Damage and Oxygen Radical Toxicity. *Science* **1988**, *240*, 1302–1309.
42. Hyslop, P. A.; Hinshaw, D. B.; Scraufstatter, I. U.; Cochrane, C. G.; Kunz, S.; Vosbeck, K. Hydrogen Peroxide as a Potent Bacteriostatic Antibiotic: Implications for Host Defense. *Free Radical Biol. Med.* **1995**, *19*, 31–37.
43. Hagansee, M. E.; Moses, R. E. Repair Response of *Escherichia coli* to Hydrogen Peroxide DNA Damage. *J. Bacteriol.* **1986**, *168*, 1059–1065.
44. Rogers, P. H.; Michel, E.; Bauer, C. A.; Vanderet, S.; Hansen, D.; Roberts, B. K.; Calvez, A.; Crews, J. B.; Lau, K. O.; Wood, A.; *et al.* Selective, Controllable, and Reversible Aggregation of Polystyrene Latex Microspheres *via* DNA Hybridization. *Langmuir* **2005**, *21*, 5562–5569.
45. Geerts, N.; Schmatko, T.; Eiser, E. Clustering *versus* Percolation in the Assembly of Colloids Coated with Long DNA. *Langmuir* **2008**, *24*, 5118.
46. Engelberg-Kulka, H.; Amitai, S.; Kolodkin-Gal, I.; Hazan, R. Bacterial Programmed Cell Death and Multicellular Behaviour in Bacteria. *PLoS Genet.* **2006**, *2*, 1518–1526.
47. Hazan, H.; Sat, B.; Engelberg-Kulka, H. *Escherichia coli mazEF*-Mediated Cell Death Is Triggered by Various Stressful Conditions. *J. Bacteriol.* **2004**, *186*, 3663–3669.
48. Hu, L. B.; Zhou, W.; Yang, J. D.; Chen, J.; Yin, Y. F.; Shi, Z. Q. Cinnamaldehyde Induces PCD-Like Death of *Microcystis aeruginosa via* Reactive Oxygen Species. *Water Air Soil Pollut.* **2011**, *217*, 105–113.
49. Chang, Q.; He, H.; Ma, Z. Efficient Disinfection of *Escherichia coli* in Water by Silver Loaded Alumina. *J. Inorg. Biochem.* **2008**, *102*, 1736–1742.
50. LaCroix, L. B.; Randall, D. W.; Nersissian, A. M.; Hoitink, C. W. G.; Canters, G. W.; Valentine, J. S.; Solomon, E. I. Spectroscopic and Geometric Variations in Perturbed Blue Copper Centers: Electronic Structures of Stellacyanin and Cucumber Basic Protein. *J. Am. Chem. Soc.* **1998**, *120*, 9621–9631.
51. Gewirth, A. A.; Solomon, E. I. Electronic Structure of Plastocyanin: Excited State Spectral Features. *J. Am. Chem. Soc.* **1988**, *110*, 3811–3819.
52. Lehninger, A. L. Amino Acids and Peptides. In *Principles of Biochemistry*; Anderson, S., Fox, J., Eds.; Worth Publishers, Inc.: New York, 1982; p 107.
53. Cuppett, J. D.; Duncan, S. E.; Dietrich, A. M. Evaluation of Copper Speciation and Water Quality Factors That Affect Aqueous Copper Tasting Response. *Chem. Senses* **2006**, *31*, 689–697.
54. Hasman, H.; Bjerrum, M. J.; Christiansen, L. E.; Hansen, H. C. B.; Aarestrup, F. M. The Effect of pH and Storage on Copper Speciation and Bacterial Growth in Complex Growth Media. *J. Microbiol. Methods* **2009**, *78*, 20–24.
55. Teoh, W. Y.; Mädler, L.; Beydoun, D.; Pratsinis, S. E.; Amal, R. Direct (One-Step) Synthesis of TiO_2 and Pt/TiO_2 Nanoparticles for Photocatalytic Mineralization of Sucrose. *Chem. Eng. Sci.* **2005**, *60*, 5852–5861.
56. Kydd, R.; Teoh, W. Y.; Wong, K.; Wang, Y.; Scott, J.; Zeng, Q.-H.; Yu, A.-B.; Zou, J.; Amal, R. Flame-Synthesized Ceria-Supported Copper Dimers for Preferential Oxidation of CO. *Adv. Funct. Mater.* **2009**, *19*, 369–377.

57. Haugland, R. P. Assaying Oxidative Activity in Live Cells with Leuco Dyes. Improved Version of H_2DCFDA. In *Handbook of Fluorescent Probes and Research Products*; Haugland, R. P., Ed.; Invitrogen: Eugene, OR, 2006; pp 754−756.
58. Myhre, O.; Andersenm, J. M.; Aarnes, H.; Fonnum, F. Evaluation of the Probes 2′,7′-Dichlorofluorescin Diacetate, Luminol, and Lucigenin as Indicators of Reactive Species Formation. *Biochem. Pharmacol.* **2003**, *65*, 1575–1582.
59. Knauert, S.; Knauer, K. The Role of Reactive Oxygen Species in Copper Toxicity to Two Freshwater Green Algae. *J. Phycol.* **2008**, *44*, 311–319.